INSTITUTE OF PHYSICS PUBLISHING JOURNAL OF PHYSICS D: APPLIED PHYSICS

J. Phys. D: Appl. Phys. **39** (2006) 4331–4336 doi:10.1088/0022-3727/39/20/007

Improvements in sensitivity and response times of photon imaging tubes

P D Townsend[1], S Hallensleben[1], M Phillips[1], R J Downey[1], R J Brooks[2], J Howorth[2] and J Milnes[2]

[1] Science and Technology, University of Sussex, Brighton, BN1 9QH, UK
[2] Photek Ltd, 26 Castleham Rd, St Leonards on Sea, Sussex, TN38 9NS, UK

E-mail: p.d.townsend@sussex.ac.uk

Received 27 January 2006, in final form 14 August 2006
Published 29 September 2006
Online at stacks.iop.org/JPhysD/39/4331

Abstract

In order to increase the transmission and speed of response of fibreoptic faceplates in imaging tubes a method is reported which used metallization only of the interfibre glass regions. This offers maximum transmission of the fibres whilst supporting high conductivity, as required for fast response times. An initial metal layer was laser ablated with light directed through the fibre array to provide a self-aligning process. Transmission has been increased threefold compared with earlier metal layer methods, which is of particular value for long wavelength sensitivity where the cathode efficiency is low. By allowing the use of more conductive pathways the more critical values of the response times have been reduced from the nanosecond to the picosecond range for these imaging tubes.

1. Introduction

In many designs of photon imaging tubes the optical image is focused onto the outer face of a fibre optic faceplate which then defines a pixel pattern of the image on the photocathode [1,2]. Emitted photoelectrons are drawn by a strong electric field to a microchannel plate electron multiplier which preserves the image information in the form of an electron beam pattern on the final collector (anode) of the detector. Alternative routes to read this output pattern are either via a position sensitive anode plate or a fluorescent screen. The fluorescent screen can be read by a CCD and then the system is described as an intensified CCD (ICCD). The device is sometimes termed a proximity focus micro-channel plate image intensifier. By switching on and off the electric field between the cathode and the microchannel plate, a high speed electro-optical shuttering action can be achieved. The tubes have an intrinsically high gain (e.g. $>10^6$) and are suitable for detection of low light level events down to the photon counting regime. These devices are easily adjustable, in terms of time resolution, over a range of exposure times from DC down to a few nanoseconds. They are consequently used in a huge variety of applications, from industrial research into auto-engines to plasma physics, chemistry, biology and through to medical diagnostics.

The minimum exposure time is limited by the CR time constant of the photocathode. The imaging area and the gap between the photocathode and the micro-channel-plate define the capacitance and so there is a compromise situation in which decreasing the gap size increases C and the CR time constant, but the closer proximity increases the resolution. The resistance of the photocathode tends to be fixed at a high value by the cathode materials, which define the spectral response, but resistance can be modified by depositing the photocathode onto a more electrically conductive substrate, albeit with a considerable loss of transmitted signal if a uniform metallic layer is used.

A major problem arises with the faster field switching since as exposure times are shortened the speed of the electrical pulse across the resistive surface of the photocathode is clearly observable on the image. If one records a time resolved sequence of images, these show how a typical photocathode is initially turned-on at the electrical contact around its perimeter, and so detection commences only at the perimeter. There is then a time delay until the central portion becomes switched-on, followed by a similar time lag until it turns off. The charging effects also modify the intensity response. Overall this can result in some intensity distortion of image information, even for tubes which are operating slower than the nominal response time set by the CR time constant. For example, in the case of detectors with a nominal 1 ns response, one can gate the recording in shorter time steps (say units of 100 ps), and then observe

apparently different images as the various sections of the detector become switched on and off. This behaviour is termed an irising effect. One must therefore avoid signal recording in time intervals faster than the time defined by the cathode response. For the normal imaging tubes, which attempt to use high optical transmission, the poor conductivity can limit the effective shutter speeds to about 100 ns for say a 75 mm diameter image intensifier, 20 ns for a 40 mm tube, 5 ns for 25 mm, 3 ns for 18 mm etc (i.e. there is roughly a linear relationship between capacitance (defined by cathode area) and the response time). There is a conflict between the requirements of fast response and image quality. The larger tubes improve resolution and can define some 12 million pixels for 40 mm diameter, or larger tubes, but the smaller tubes enable faster shutter speeds, albeit with lower spatial resolution. For the smaller tubes, with the best time resolution, definition is limited to no better than 1–2 million pixels. Some early 'fast shutter' image intensifier designs incorporated a photocathode built on a semi-transparent metallic under layer and for small sized (18 mm) imaging tubes, using a thick nickel underlay below the photocathode, resulted in a ∼50% transmission, and cited irising times reduced to ∼100 ps [3–6]. Thicker metallization increases response speed, but at the expense of optical transmission. There have been a variety of approaches using patterned grid or line structures which can simultaneously increase both conductivity and transmission, without degrading the response times. Whilst these schemes offer major benefits they are still somewhat undesirable in terms of optimized image quality since fibreoptic faceplates do not have long range periodicity in the placement of the fibres, and different sections are randomly aligned relative to the deposited grid patterns [3–8]. Typically, mesh underlays allow an order of magnitude improvement in exposure time, but the procedure for making a mesh underlay involves application of photo-resist, exposure through a mask, removal of unexposed photo-resist and a final removal of exposed photo-resist and metallization steps. It is consequently expensive and prone to defects. The practical challenge is to raise the conductivity even further with a grid which aligns with the fibres, and to do so without blocking the incident light. Such an approach is described in this current work.

One notes a recent and major opportunity for the use of fast response imaging tubes is in biological applications as there are many excellent examples of lifetime resolved imaging to differentiate healthy and cancerous cell types using luminescence decay from signals at the tissue surface [8–11]. Many of these examples use short wavelength excitation and gated imaging detectors to resolve signals on the 10 to 100 ps time scale. In these cases the signals are often at wavelengths where the quantum efficiency of the photocathodes is high. A much more challenging situation exists for *in vivo* optical detection of breast cancer as in this application the cancer sites can be buried deeply below the surface. The proposed solution is to use pulsed lasers in the wavelength range near 800 nm, where tissue is transparent. Unfortunately it is also the spectral range where the cathodes are least efficient [1, 2, 12], so high transparency fibre optic faceplates are essential. For breast cancer detection, time delays occur in detecting the laser pulses that are scattered from cancer sites. Data resulting from changes in scattering at a cancer site to different detector positions can be used to identify the scattering site and its dimensions. Variations in wavelength can help to differentiate between cancerous and non-cancerous sites, such as cysts. It is essential to make this optical detection and site location when the cancerous regions are at a very early stage, of just a few millimetres. Such precise location of these small scattering objects inevitably implies that the response times must be as short as a few tens of picoseconds. The widespread incidence of breast cancer (e.g. in ∼10% of women) is therefore a key reason for developing faster response is timing requirement for spatial resolution of laser pulsed scattering from early stage breast cancer. As already mentioned, the cancer problem is particularly challenging as it requires high sensitivity to wavelengths where tissue is transparent, around 800 nm, and a spatial resolution of around a millimetre (i.e. <10 ps timing).

There have been many suggestions on routes to improve the cathode sensitivity in this spectral range [12, 13] and the current results describe an alternative simple processing method for metallization of the fibreoptic faceplates which resolves some of the previous problems so as to allow maximization of the red sensitivity and response times on the tens of picosecond timescale.

2. High conductivity faceplates

To increase photocathode response speed by increasing the thickness of a continuous metal substrate layer is not a realistic option as the metal blocks the incoming light. Similarly, conduction via the photocathode material, typically the S20 multialkali layer for the red sensitive tubes, is inadequate, since the cathode is thin and of low conductivity. The alkali and antimony photocathodes are relatively poor conductors, and are typically only 30 to 100 nm thick. For example, the multialkali S20 cathodes have a resistance of $\sim 10^7$ ohms per square and the bialkali types (S11 or S13) are worse at $\sim 10^{10}$ ohms per square [2]. With a transmitting metal underlay the values still only rise to give a resistance of some hundreds of ohms per square. Additionally, there are limitations in the selection of the metal suitable for underlays, as they must both bond to the glasses of the window and not degrade the photocathode efficiency. In order to move from the nanosecond to the picosecond response range, the resistance needs to fall to ∼5 or 10 ohms per square. As mentioned, patterned thick metallic grid layers on the faceplate offer considerable benefits, but for good image quality lines and grids are undesirable, as the fibreoptic faceplates do not have any long range periodicity in the placement of the fibres and different sections are randomly aligned. Therefore, even very fine line metallic grid patterns are superposed on the images and randomly cross over the fibre ends.

3. Laser ablation of metallic fibre coatings

To overcome these problems we proposed a very simple solution in which a conductive metal layer is deposited uniformly across the face plate and then metal is preferentially removed only from the ends of the transmitting fibres using a self-aligned laser ablation technique. This processing retains metal on the interface glass between the fibres which, in image terms, is dead space. The main advantage of metallization

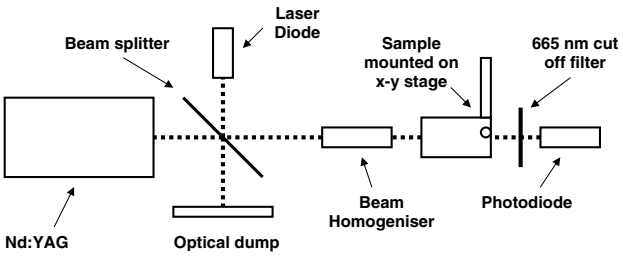

Figure 1. Schematic of the laser ablation system. During ablation the pulsed laser is directed via a homogenizer onto the outer face of the coated fibreoptic window. The laser pulses are transmitted through the fibreoptic to ablate metal only from the end of the fibre, and not from the interfibre regions. Transmission measurements are made via a longer wavelength laser diode passing through the window and cut-off filter to a detector to monitor the progress of the ablation.

of only the interfibre glass is that one can then achieve high conductivity from a metallic pattern that does not block the optical power. Further, this patterning allows the quantum efficiency of the cathode to be maintained at a maximum value, whilst the response speed can be increased. In our initial laser processing step the pattern has been produced with relatively thin metallic layers. This gives a template for further metallization. As a second stage, two successful variants on routes to increase the conductivity from the first patterning step were demonstrated. In the first method the process was repeated to build up the metallic thickness in several deposition and laser ablation steps. A second approach was to form the initial laser ablated mask pattern in a metal which bonds firmly to the faceplate glass, and then to electroplate a second metallic layer to raise the conductivity further. Typically this involved chromium or nickel for the ablation stage, followed by electroplating with copper. Once the requisite high conductivity pattern has been developed then the normal photocathode deposition and processing can proceed.

The basic challenge is to only remove the metal from the ends of the randomly arranged pattern of fibres. The solution used here is to metal coat the faceplate on the side where the cathode will eventually be deposited. An intense laser beam is used to illuminate the non-metallized face and the transmitted light therefore reaches the metal only at the ends of the fibres. Laser pulses can then ablate the metal from the ends of the fibres. By directing the laser onto the outside of the faceplate the fibres automatically act as an alignment mask, even for a random fibre packaging. Figure 1 sketches the geometry of the laser ablation and monitoring setup.

Metals which bond to the faceplate must also be compatible with the subsequent cathode deposition and this limits the choice of material. In the present case, films of nickel were found to be satisfactory. Nickel was also a suitable substrate for electroplating of copper to increase the conductivity before the cathode stage. The ablation conditions depend on the thickness of the metal layer and pulses were typically derived from a laser beam operating in the range of 50 to 200 mJ per pulse. The initial beam profile was homogenized to some extent, and after transmission through the face plate, the beam delivered pulses with energy densities in the range of 50 to 200 mW cm^{-2} at the metallized side of the faceplate. The pulses were generated at 532 nm from the harmonic of

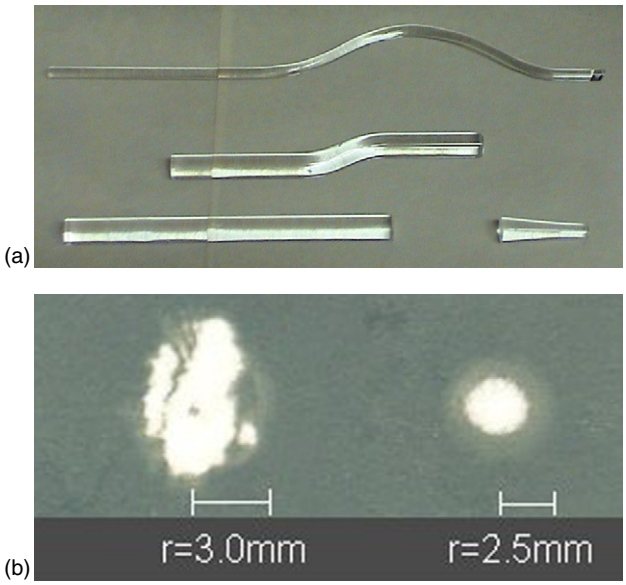

Figure 2. (*a*) Examples of silica rods and cone type beam homogenizer. (*b*) Images of the Nd : YAG beam before and after homogenization.
(This figure is in colour only in the electronic version)

a pulsed Nd : YAG laser operating at 10 Hz, and with a pulse duration of ∼5 ns.

Initially the laser pulses were too poorly defined for the present purposes, being non-uniform in intensity across the beam profile. In addition, there were some >10% intensity variations between pulses. The coverage of the laser beam was typically only a few millimetres in cross section and therefore it is necessary to mechanically step the ablation area across the surface of the faceplate, which in the current examples were 50 or 70 mm in diameter. It is essential to use a homogeneous ablation beam with sharply defined boundaries. To generate suitably homogeneous beam intensity uniformity was achieved very simply by internal scattering within a silica rod or cone. Figure 2(*a*) indicates alternatives which all showed improvements in beam uniformity. The best results were achieved with the tapered cone. After prolonged usage the bent rod structures tended to eventually show silica damage near the bends. Such damage may arise from internal focusing or stress retained from bending the silica. Figure 2(*b*) records the initial and final pulse intensity patterns. The output beam impinged on a metal aperture in front of the fibreoptic faceplate. As shown below, this not only resulted in good ablation uniformity but also defined the boundary within a few fibre pixels. The target window was stepped in front of the beam to scan the entire faceplate. This gave uniform metal removal from the fibre ends of the faceplates. Subsequent electroplating and/or cathode deposition within a detector was then made.

To offset the problem of pulse power variations the ablation was performed with several low power pulses, rather than attempting to remove all the fibre end metal in a single shot at high power. As shown by figure 3, the pattern of metal removal from the fibre ends was not uniform across the fibre. This was expected as the inherent optical power distribution of the guided light defines a maximum intensity in

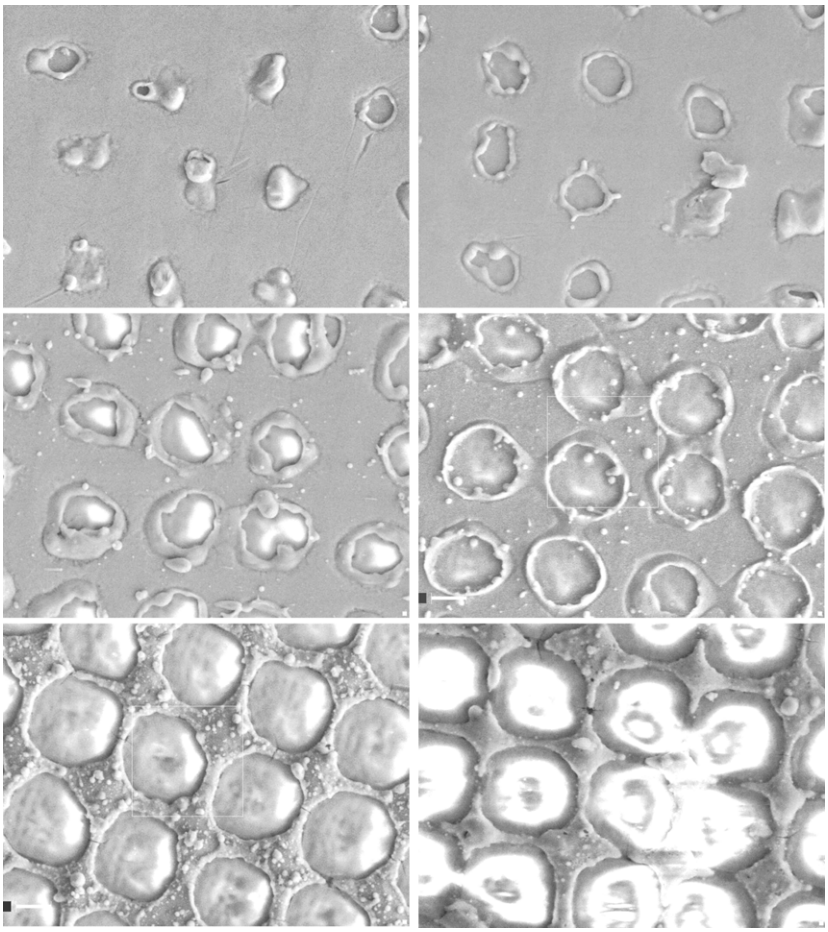

Figure 3. Examples showing the development of the ablation of metal from the fibre regions as the result of laser pulses with increasing power. Note the initial ablation removes metal from the centre of the fibre.

the centre of the fibre. Therefore just above the metal ablation threshold a central hole appeared in the coating, and this could be expanded in a controlled fashion by subsequent pulses. For complete clearance of the fibre end, 5 to 10 pulses were typically used. The development of coating ablation pattern is shown in figure 3 as a function of pulse energy. The figure presents a series of SEM images for ablation with increasing laser energy for Photek faceplates with 250 nm of Cu on a 30 nm Cr bonding layer. Ablation starts in the centres of the fibre cores and moves outwards. At the earlier stages there is temporarily a molten fringe of metal around the ablated holes. For the highest power level (bottom right) the grid has been broken, resulting in charging of the insulating faceplate in the electron beam of the SEM (white areas). Other copper effects will be discussed below.

Nickel was the preferred coating layer and for a 70 nm nickel film the threshold required a total laser pulse power of ∼50 mJ (NB prior to homogenization). Lower powers were adequate for thinner films (e.g. the threshold dropped to ∼30 mJ for a 20 nm Ni film). With low power pulses it was possible to control and follow the development of ablation from the fibre centre out to the edge. Further pulses were undesirable as the scattered light caused ablation of the coating on the interface region.

In principle the ablation could be achieved in a single shot but this would require prior knowledge of the power level that matched the particular coating thickness and bonding quality. Except at the very highest power levels, and/or with many multiple shots, the laser pulses had a minimal effect on the materials of the fibre-optics. Very high power levels are thus undesirable, as they not only remove the fibre coating, but also scatter and seriously degrade the interfibre metal cladding. In some cases there was evidence of damage to the ends of the fibres when the single shot approach was used. In fact, this would not be a serious problem, as having a non-planar fibre end, which is coated with cathode material, can in principle result in improved cathode quantum efficiency [13]. The ablation power levels are sensitive to the glasses of the faceplates, the metal used and the thickness and bonding of the metallization. Therefore it was necessary to have *in situ* monitoring of the faceplate transmission and transmission and ablation were controlled during a sequence of laser shots.

Online monitoring of the optical transmission of the faceplate was arranged as shown in figure 1. A low power red laser diode was used to send a signal along the same axis as the ablation laser. The red beam passed through the faceplate and a green blocking filter to a red detector diode. It was then possible to follow the development of the ablation process and end it before the scattered light impaired the adhesion of the interfibre metal. In the monitoring mode a shutter arrangement blocked the reflections of the 532 nm pulse from returning to

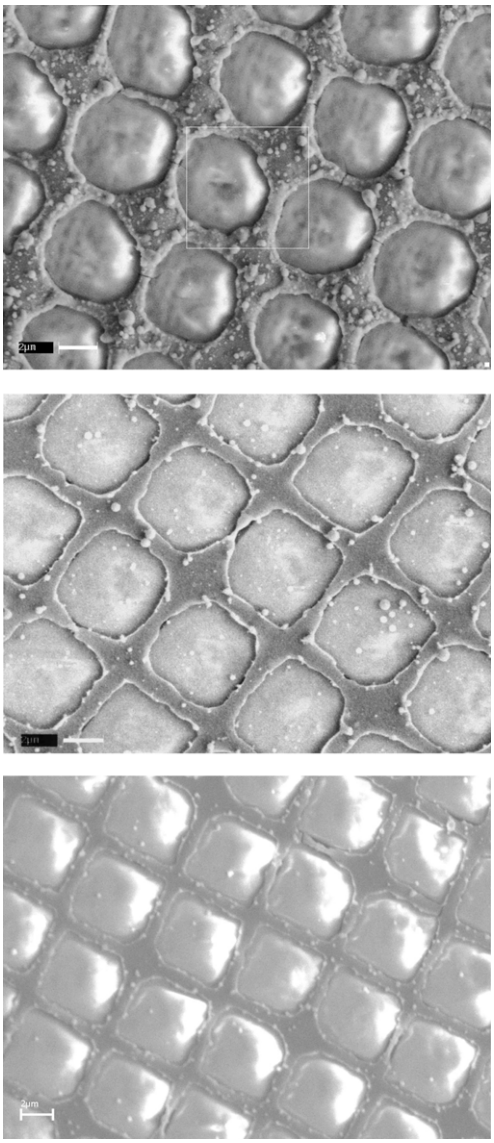

Figure 4. Ablation patterns where metal has been removed from the ends of the fibres but metal has been retained on the interface glass.

the red laser diode, since such reflected pulses could destroy the diode laser.

Several types of fibreoptic faceplates have been used with core and cladding glasses of different compositions. The method has worked well in all cases (i.e. with faceplates from different suppliers and various compositions). Figure 4 shows three examples of the success of the ablation technique in removing metal preferentially from the fibres, whilst retaining metal on the interfibre glass. In the first example of figure 4 the metal layer was built up from a 5 nm Cr underlayer, to provide good metallic adhesion to the glass, plus a 50 nm thick Ni layer. The figure shows a nominally square ablated pattern or $\sim 5\,\mu$m opening with interfibre metal coating of $\sim 1\,\mu$m width.

Figure 5(*a*) shows the boundary zone between an ablated and non-ablated region. The coated, but non-ablated, zone on the left-hand side of the image clearly reveals the pattern of the fibres that are arranged in blocks of 2×2. In the corners of each block there is a darker patch which corresponds to

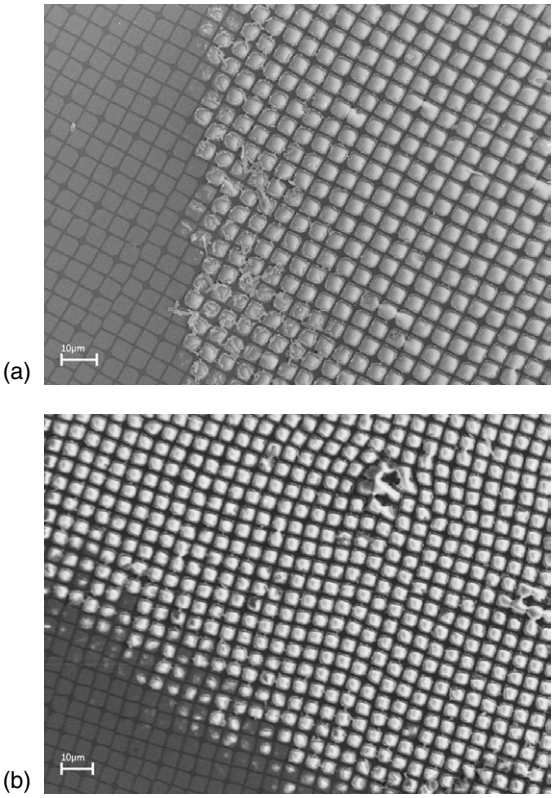

Figure 5. (*a*) A boundary zone between coated material (left side) and exposed glass as the result of ablation (right side). Note the boundary zone is tightly confined as the result of beam homogenization. (*b*) As for figure 5(*a*) but this example also demonstrates the inherent misalignment of the blocks of fibre optic material.

an interface absorber glass. The ablated zone has a uniform pattern of exposed fibre ends, where the metal has curled away from the surface. At the boundary between ablated and coated fibre there is a ragged pattern which extends over just a few fibre widths. Figure 5(*b*) shows a similar discrimination between coated and ablated fibre ends. In the ablated region the non-periodic arrangement of fibres is visible within this image. In this case the blocks of fibre slightly misalign and resemble a classical view of a crystalline dislocation line. In other examples the fibre blocks can be totally misaligned. The building block structure of the faceplate has inherent distortions and imperfections which are reflected in the ablation pattern.

In the case of the nickel coated faceplates it was possible to achieve optical transmission of more than 90% of that of the uncoated window. This is a threefold improvement in transmission compared with examples from the former overall metallization approach. The second objective, to increase the conductivity, has also been achieved and the conductivity has been raised to $\sim$10 ohm per square. This value is reflected in the faster response times of imaging tubes. Measured response times were better than $\sim$500 ps, but assessment of faster responses was not possible due to limitations of the available test equipment.

In addition to the use of nickel, other metals have been considered. As mentioned, copper has been electroplated on the nickel to raise the conductivity. We also considered

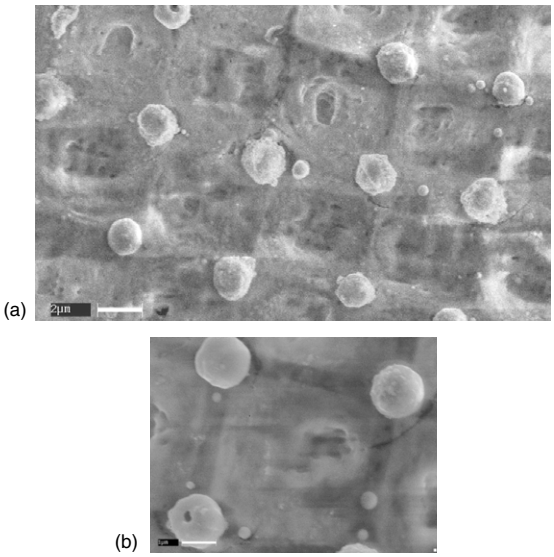

Figure 6. An example of a copper ablated surface in which the copper has melted and formed into spheres as the result of surface tension.

the option of commencing directly with a copper coating. In practice this is not an ideal approach as it appears that on many occasions the ablated copper had also undergone a melting phase of the material situated in the interfibre zone. Figure 6(*a*) shows an interesting example with a copper coated faceplate in which, during the use of a high power pulse, there had obviously been melting of the copper along the boundary zone, and there is evidence at this maximum power level of some fibre glass damage. The surface tension of the molten copper has pulled the metal into the form of copper spheres at the corners of the fibre zones. There are also smaller spheres evident along the boundary lines, as seen in figure 6(*b*). In principle this might offer some information on the transient temperature reached by the metal. For large particles one assumes that the copper has melted at the normal melting temperature (1,083 °C). Nevertheless, melting need not necessarily imply that the normal melting temperature of copper had been reached as the film thickness, fibre dimensions and resultant copper spheres include features on the sub-nanometre scale, and the melting point of metals often strongly decrease as the particle size is reduced. For example, data are available for a comparable metal, gold, in which the bulk melting point falls from 1,064 °C down to 830 °C for 2 nm diameter regions and even lower to 350 °C for 1 nm particles [14, 15].

4. Conclusion

The preceding figures are a demonstration that metallization and preferential ablation from the fibre ends is achievable and this is compatible with cathode deposition on fibreoptic plates. The method is simple to implement and the faceplate transmission rises to >90% of the normal uncoated value, (i.e. as needed for a high quantum efficiency of the device, especially at long wavelengths). Metal remains in the regions between the fibres and thick layers of nickel, or nickel subsequently electroplated with higher conductivity metals, results in conditions where the conductivity can be increased to just a few ohms per square. This is essential for the operation of fast photon imaging tubes. In the present examples the response times were at least as fast as ∼500 ps, which was the speed limit set by the available test equipment. The existing literature suggests that reduction to a few ohms per square should form devices that can function considerably faster.

Acknowledgments

We thank the European Commission for support with funding from the programme IMPECABLE, Contract Number G5RD-CT-2000-00372.

References

[1] www.hamamatsu.com; www.photek.com; www.photonis-dep.com; www.proxitronic.de
[2] 1994 Photomultiplier tubes, principles and applications *Philips Photonics Manufacturers Manual (Photonis series)*
[3] King N SP, Yates G J, Jaramillo S A, Ogle J W and Detch J L 1981 *Proc. SPIE* **288** 426
[4] Thomas S W and Trevino J 1990 *Proc. SPIE* **1358** 84
[5] Thomas S, Shimkunas A R and Mauger P E 1990 *SPIE* **1358** 91
[6] Hoess P and Fleder K 1999 *Proc. SPIE* **3783** 194
[7] Dowling K, Hyde S C W, Dainty J C, French P M W and Hares J D 1997 *Opt. Commun.* **135** 27
[8] Dowling K, Dayel M J, Lever M J, French P M W, Hares J D and Dymoke-Bradshaw A K L 1998 *Opt. Lett.* **23** 810
[9] Dowling K, Dayel M J, Hyde S C W, French P M W, Lever M J, Hares J D and Dymoke–Bradshaw A K L 1999 *J. Mod. Opt.* **46** 109
[10] Lévêque-Fort S *et al* 2002 *J. Fluoresc.* **12** 279
[11] Tadrous P J, Siegel S, French P M W, Shousha S, Lalani E-N and Stamp G W H 2003 *J. Pathol.* **199** 309
[12] Townsend P D 2003 *Contemp. Phys.* **44** 17
[13] Townsend P D, Downey R, Harmer S W, Wang Y, Cormack A, McAlpine R and Bauer T 2006 *J. Phys. D.: Appl. Phys.* **39** 1525
[14] Buffat P and Borel J-P 1976 *Phys. Rev.* A **13** 2287
[15] Cortie M B 2004 *Gold Bull.* **37** 12